ELSEVIER

Journal of Power Sources 85 (2000) 203–211

JOURNAL OF POWER SOURCES

www.elsevier.com/locate/jpowsour

Performance parameters of material studies for AMTEC cell

M.A.K. Lodhi *, A. Daloglu

Department of Physics, Texas Tech University, Lubbock, TX 79409 USA

Received 24 May 1999; accepted 10 June 1999

Abstract

In the recent past, a number of programs have focused on developing AMTEC technology associated with its fabrication and design. The performance level, however, achieved to-date is below the theoretical potential of this device. For improving performance characteristics we examined the sources of power loss and proposed some solution which are demonstrated with computer calculations. Two kind of losses that reduce efficiency are thermal (as a result of thermal conduction and radiation of materials) and electrical (related to the ohmic resistance of material). Each of the losses can, in principle, be reduced separately by varying current in the load. To reduce the thermal losses, the current must be increased; to reduce the electrical losses, the current in the load must be decreased. In such inversely competitive situation, an optimum value must be sought which has been achieved by applying the optimization theory. Heat losses due to radiation are reduced by increasing the current density and by reducing the emissivity of electrodes and other surfaces. Changing of some of the materials used in the cell has proved to be helpful in improving the cell performance. As a result of this overall effort, we have been able to demonstrate the improvement in the efficiency of AMTEC cell by 77%.

Keywords: Thermal-to-electrical conversion; Power loss; Optimization; Efficiency

1. Introduction

A power system considered for a number of potential space missions requires long life, high specific power (power/mass), that is low mass, high areal power density (power/area), high efficiency, low cost and static in operation. To a great extent a system called Alkali Metal Thermal to Electric Converter (AMTEC) does possess latent qualities that would qualify it to be a possible candidate for space power. It can provide efficiency close to the theoretical Carnot efficiency at relatively low temperatures. AMTEC has conversion efficiency much higher than other direct thermoelectric devices. An optimized AMTEC can potentially provide a theoretical efficiency when operated between 1000 K and 1300 K on the hot side and between 400 K and 700 K on the condenser side. It is fuel source insensitive. It can utilize heat as input fuel from most of any source like fossil fuel, the Sun, radioisotopes, or the nuclear reactor. AMTEC, with solar energy as a heat source, is capable of being an alternative to photovoltaic-based power system for use of low earth orbit (LEO) for future NASA and Air Force missions. It is intended to be used for future NASA missions like Pluto Express (PX) and Europa early in the millennium 2000 with radioisotope decay as its heat input.

Since the mid-1960s, a number of programs in developing the operating principle, design and technology of AMTEC have been evolving rapidly. Kummer and Weber [1] demonstrated the conversion of heat, through the sodium cycle, into electricity by the use of beta″-alumina solid electrolyte (BASE) in a patent assigned to Ford Motor in 1968. Several years later, Weber described the operating principle of AMTEC with a liquid anode in a historical paper in 1974 [2]. It took some time for the community to recognize the potential qualities of AMTEC with regard to its uses and application for terrestrial and space power. Accordingly, there was not much activity in modeling, design and technology development of AMTEC until almost the beginning of 1990s. During that AMTEC dormant period, there were few landmark papers primarily on its principle and working efficiency [3–7]. A review article on the progress of thermionic technology during a 10-year period of 1983–1992 covers the slow moving development in AMTEC technology during that period [8]. The use of nuclear power, from the radioisotopes or nuclear reactors,

* Corresponding author. Tel.: +1-806-7423767; fax: +1-806-7421182; E-mail: b5mak@ttacs.ttu.edu

0378-7753/00/$ - see front matter
PII: S0378-7753(99)00335-3

for the space pointing out the potential use of AMTEC perhaps provided another motivation in looking for its application [9–11]. A flurry of AMTEC activities began with a great vigor around the world at the beginning of the 1990s. NASA Lewis Research Center (LeRC) has an interest in developing thermal energy storage (TES) for the solar dynamic ground test demonstration (SDGTD) program. The research and development effort at Jet Propulsion Lab (JPL) included studies, which address both overall device construction and investigation into the AMTEC components [12–25]. Advanced Modular Power Systems (AMPS) have been focusing on designing and manufacturing AMTEC cells for the PX mission [26,27]. The Air Force Research Lab (AFRL) has an interest in developing an electrical power system for the payload in LEO for a duration of 5 years and in testing the performance of AMTEC for the PX [28–30]. Orbital Science has been conducting a series of studies of radioisotopes power system based on general-purpose heat source (GPHS) for potential deep space missions [9,31–33]. AMTEC has been found compatible with direct conversion from the projected SP-10 nuclear space power reactor [10,11].

Recently, the University of New Mexico has been engaged in modeling and analysis of AMTEC performance and evaluation [34]. In Japan, the interest in AMTEC analysis has evolved at Kyushu University in collaboration with Electrotechnical Laboratory [35,36]. Creare has primarily concentrated on evaporator component of AMTEC to enable it to operate efficiently [37–39].

While these programs resolved a number of key technological issues associated with the design and fabrication of AMTEC successfully, the performance level achieved hitherto is still below the theoretical potential of this device. In tracking down the source of power loss during the test cell performance of various AMTEC designs, the major losses are found to be radiative and conductive. Since the cell is tested in vacuum there is no convective loss. Most of the heat escapes through the cell wall. There are radiative losses due to condenser and along the artery as well. In order to minimize these losses we propose to use some different materials which should be compatible with the operating conditions of the cell and capable of reducing these losses. We select a test AMTEC cell designated by PX-3A, which has been in operation at AFRL since July 9, 1997 and compare its theoretical performance as a function of the variation in the material parameters.

2. Principle and working of AMTEC cell

A typical AMTEC cell is shown in Fig. 1 schematically. An AMTEC cell is a static device for the conversion of heat to electricity performing two distinct cycles: (1) conversion of heat to mechanical energy via a sodium-based (or any suitable alkali metal) heat engine and (2) conversion of mechanical energy to electrical energy by utilizing

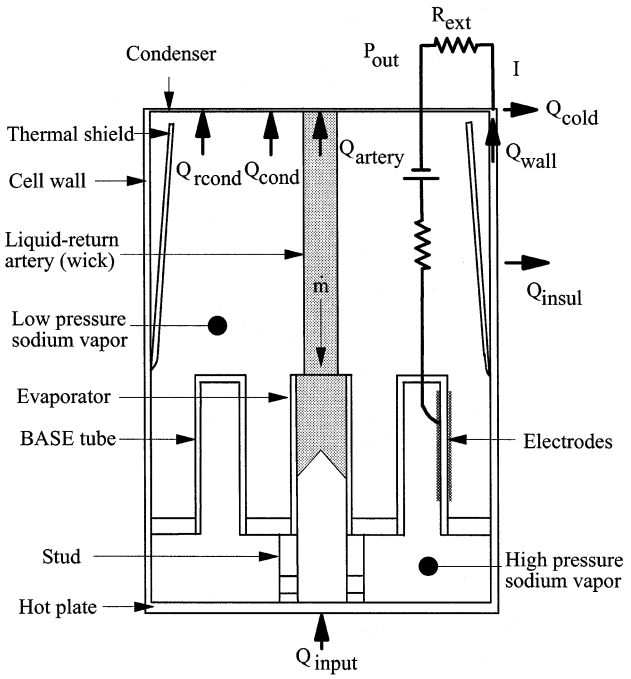

Fig. 1. A schematic diagram of vapor-anode AMTEC cell.

the special properties of the BASE material. It has the potential for reliable long life operation and high conversion efficiency. The general principles governing the operation of an AMTEC cell have been given quite elaborately in the early stages of its development [1–5]. The essential thermodynamic aspects of the sodium-based engine have been described in those references. Accordingly, a brief outline will be presented here for the self-consistency of this work.

AMTEC, a relatively new type of device, is based on the principle of a sodium concentration cell, conceived in the late 1960s [1–4]. A closed vessel is divided into a high temperature, high-pressure region in contact with a heat source and a low temperature, low pressure region in contact with a heat sink. A barrier of a BASE sheet whose ionic conductivity is much larger than its electronic conductivity separates these regions. The BASE is coated with a porous metal electrode (cathode) which covers the low-pressure surface of the BASE. A closed container is partially filled with a small quantity (typically < 10 g) of liquid sodium as the working fluid. Sodium ions disperse through the BASE in response to the pressure differential (gradient of Gibbs free energy). Electrical leads are connected with the porous cathode and with the high temperature liquid (vapor) sodium, which acts as the anode. When the circuit is closed electrons flow to the porous anode surface through the load, producing electrical work. A return line and electromagnetic pump or a wick circulates the sodium from the cold zone (condenser) to the hot zone (heater) of AMTEC. It is limited to 1350 K because of sodium interaction with the BASE. The lower temperature region is limited to a minimum of 500 K by the need of

maintaining the sodium in the liquid state (but it would be operating around 623 K for high efficiency). As the condenser temperature increases above 700 K the efficiency decreases [3].

The main component of an AMTEC cell is the BASE tube which essentially conducts sodium ions much more rapidly than what it does for neutral sodium atoms or negative particles like electrons. A sodium pressure difference across a thin BASE tube drives sodium ions from the high-pressure side to the low-pressure side. Thus, positively charged sodium ions concentrate on the low-pressure side while negatively charged particles, electrons remain concentrated on the high-pressure side (inside the BASE tube), resulting in an electrical field gradient across the BASE tube. This gradient balances the sodium pressure differential, thus preventing the further flow of sodium ions. This electrical potential difference is utilized to drive an electric current through a load by applying some appropriate electrodes at the two ends of the tube. The unusual properties of the BASE provide a method of converting the mechanical energy, represented by the pressure differential, into electrical energy. Or in other words, the BASE converts a chemical potential difference into an electrical potential difference. As the electrons, after going through the load, reunite with sodium ions they form neutral sodium atoms in the vapor state on the low-pressure side. The sodium vapor travels to the condenser where it condenses into liquid state. The sodium liquid is pressurized through a wick or electromagnetic pump and is returned to the high-pressure side of the BASE. In that way, the thermal-to-mechanical-to-electrical conversion process is completed. The efficiency of this final conversion is governed by variety of irreversible kinetic and transport processes occurring at the electrode interfaces, within the BASE material, internal impedance, and thermal conduction and radiation losses [12–14]. A number of efforts are underway to develop practical and high efficiency cells [18,40–45]. AMPS, in collaboration with AFRL, has been manufacturing and testing for improving efficiency of PX series of AMTEC cells [26–30]. The latest multi-tube AMTEC cells have been in operation for some time. The longest in operation among them is PX-3A whose parameters are given in Table 1. We have modified it theoretically for improving efficiency by varying parameters governing its material properties for optimum conditions in a computer model of the cell to predict its performance.

Table 1
Design parameters of PX-3A cell

Cell diameter (mm)	31.75
Cell height (mm)	101.6
Evaporator type	Deep Cone
Evaporator elevation (mm)	5.18
Evaporator standoff thickness (mm)	0.71
Evaporator standoff material	SS
Standoff rings (mm)	1.1
Rings material	Ni
Stud area (mm^2)	38
Stud material	SS
Number of BASE tubes	5
Tube length	32
Electrode/tube (mm^2)	600
Tube braze material	TiNi
Current collector	60-mesh Mo
Feedthrough braze	TiCuNi
Radiation shield type	Circular
Shield material	SS
Condenser type	Creare
Hot side	SS
Cell wall	SS
Initial test date	7/9/97
Operation (h)	4500

3. AMTEC theory and analysis

The transport of sodium through an AMTEC cell is a complex phenomenological process. Its exact detailed analysis is very difficult and is further complicated as it requires the simultaneous solution of thermal, fluid flow, and electrical equations. Those equations are interdependent, with each of the three analyses requiring the results of the other two. This interdependence is between a number of axially varying distribution functions. (Had it been between single-valued variables; it could have been solved by a set of simultaneous algebraic equations.) Specifically, solving for the cell's temperature distribution requires the knowledge of the axial variation of the sodium flux through the BASE tube and of the electrical output power density profile over the tube length. Solution of the axial pressure variation of the low-pressure sodium requires knowledge of the cell's temperature distribution and the BASE tubes' current density variation. Similarly, solving for the axial variation of the current density and of the inter-electrode voltage requires prior solution of the axial variation of the BASE tube temperature and internal-to-external pressure ratio. Those interdependent distribution functions require solutions of coupled differential and integral equations by a more sophisticated procedure. Schock et al. [32] generated a thermal analysis model for multi-tube AMTEC cell by appropriately modifying the ITAS and SINDA codes [46,47].

Energy conversion devices have few equilibria and are typically open systems unlike the classical thermodynamics which is restricted to reversible and closed systems. Onsager's treatment of irreversible processes, such as diffusion, can be applied to AMTEC operation to deal with its irreversibility of the process and openness of the system [48]. One can write, in principle, the effective emf, V as a function of cell voltage in open-circuit, V_{oc} and electrode polarization over potential, $V_{op} = (\zeta^a - \zeta^c)$ [2] from Nernst equation [5]. The open-circuit voltage and charge-exchange

current density are related with the cell temperature and pressure [19]. We can thus write for the net power output as:

$$P_{out} = VI, \quad (1)$$

where

$$V = V_{oc} - JR_{int} - V_{op}, \quad (2)$$

$$V_{oc} = RT_B/F \ln P_a/P_c, \quad (3)$$

R is the gas constant = 8.314 J/mol K. T_B is the temperature of the BASE tube, P_a and P_c are the pressures at the anode and cathode sides respectively. I is the net current in the circuit and R_{int} is the total internal resistance of the cell including the contact resistance of the electrodes $R_{contact}$, sheet resistance in the plane of electrodes R_{sheet}, resistance of the current collectors $R_{collector}$, resistance of the bus wires and conductor leads to the load R_{bus}, the resistance for charge exchange polarization losses at the BASE-electrodes interfaces R_{op}, and the BASE ionic resistance, R_B given by:

$$R_B = \rho_B t_B. \quad (4)$$

where ρ_B and t_B are electrical resistivity, the expression for which has been developed by Steinbruck et al. [49], and the thickness of BASE tube, respectively. R_{int} will be written here as the sum of the terms in the same order as stated above:

$$R_{int} = R_{contact'} + R_{sheet} + R_{collector} + R_{bus} + R_{op} + R_B \quad (5)$$

4. Heat losses

For a multitube AMTEC cell, the heat losses are shown in Fig. 1. Most of the heat passes the cooling fluid (air) through the condenser. The heat passes the cooling fluid,

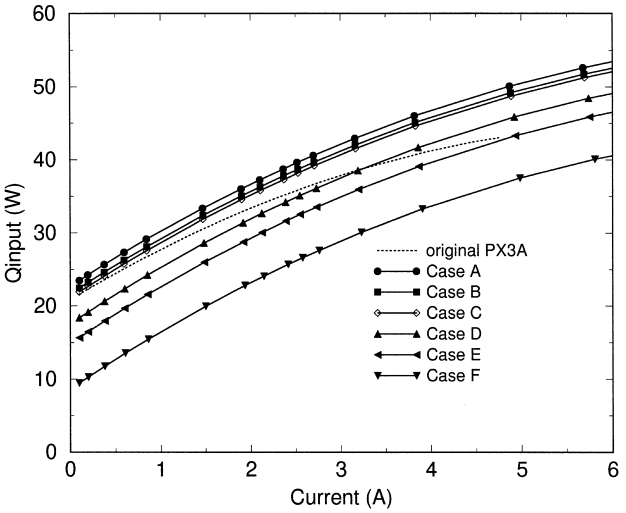

Fig. 3. The heat supplied to the AMTEC cell.

Q_{air}, is the result of heat conduction, heat radiation and condensation of vapor sodium as:

$$Q_{air} = Q_{wall} + Q_{artery} + Q_{rcond} + Q_{cond} - Q_{cold} \quad (6)$$

where Q_{wall} is the conducted heat to condenser through the cell wall, Q_{artery} is the conducted heat through the artery, Q_{rcond} is the net radiated energy between the condenser and other surfaces, Q_{cond} is the latent heat of condensation of sodium, and Q_{cold} is the heat conduction loss at the edge of cold plate. These heat losses can be expressed in the following expressions:

$$Q_{wall} = -k_{wall} A_{wall} (dT/dx)_{x=\text{at condenser}} \quad (7)$$

$$Q_{artery} = -k_{artery} A_{artery} (dT/dx)_{x=\text{at condenser}} \quad (8)$$

$$Q_{cond} = h_{fg} \dot{m} \quad (9)$$

where k is the thermal conductivity, A is the area, h_{fg} is the latent heat of condensation of sodium per unit mass

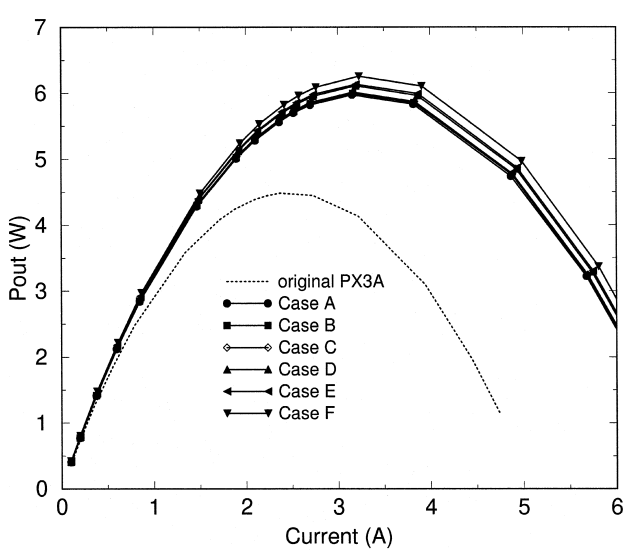

Fig. 2. The electrical power generated by the AMTEC cell.

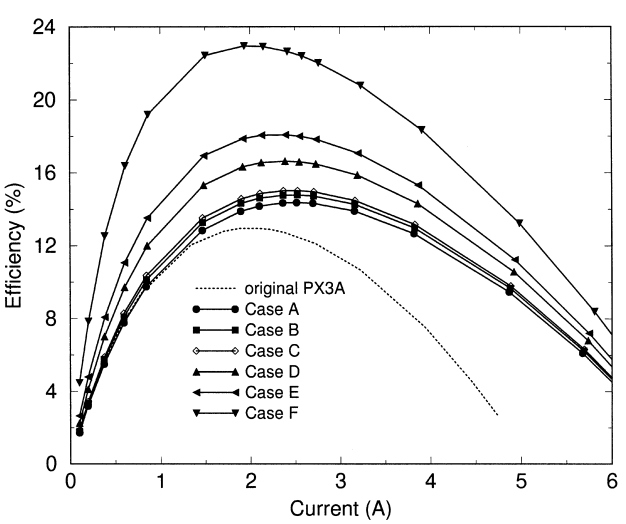

Fig. 4. The cell conversion efficiency.

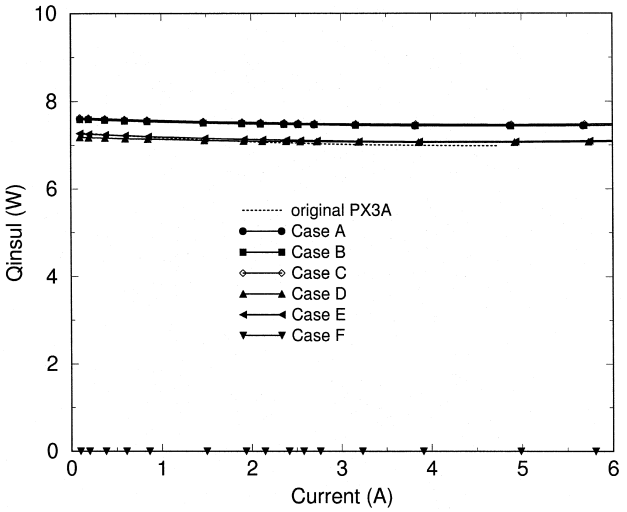

Fig. 5. Heat losses to ambient through cell wall and insulation.

and $\dot{m}$ is the sodium flow rate. For wall and artery, $\mathrm{d}T/\mathrm{d}x$ is the temperature gradient at the condenser. As an enclosure, every surface in the cell affects heat radiation. Net radiated energy between the condenser and other surfaces depends on view factors F_{ij}, emissivities ε_i, and temperatures T_i for every surface, so it can be expressed as

$$Q_{\mathrm{rcond}} = f(\varepsilon_1, \varepsilon_2, \varepsilon_3, \ldots, T_1, T_2, T_3, \ldots, F_{11}, F_{12}, F_{13}, \ldots) \tag{10}$$

Some heat goes to ambient through cell wall and insulation, and it can be given as

$$Q_{\mathrm{insul}} = \int_{x=0}^{x=\text{cell length}} K(x)\, P\left[T_{\mathrm{wall}}(x) - T_{\mathrm{insul}}(x)\right] \mathrm{d}x \tag{11}$$

where $K(x)$ is some constant which includes conduction and radiation effects, and P is the perimeter of the cell wall. T_{wall} and T_{insul} are cell wall temperature and insulation temperature, respectively, which change along the cell length. Heat conduction loss at edge of cold plate, Q_{cold}, can be calculated similar to Q_{insul} taking temperature T_{cond} instead of T_{wall}, but Q_{cold} is small. The total of heat losses become

$$Q_{\mathrm{loss}} = Q_{\mathrm{air}} + Q_{\mathrm{insul}} + Q_{\mathrm{cold}} \tag{12}$$

The overall conversion efficiency of AMTEC cell is given by [5,50]:

$$\eta = P_{\mathrm{out}}/Q_{\mathrm{input}} \cong VI/\left[VI + Q_{\mathrm{loss}}\right] \tag{13}$$

In order to get the maximum efficiency, the total heat losses, Q_{loss}, must be minimum. This implies that:

- The choice of working fluid be such that its latent heat of condensation must be low.
- The emissivities of materials used for BASE tube, outer condenser surface, outer artery surface, inner cell wall and radiation shields must be low for minimizing radiation losses.
- For conductive losses through the wall, artery and insulation, low thermal conductive materials must be used, but for hot plate high thermal conductivity material must be used.
- The output power maximizes when the load resistance is equal to the internal resistance of the cell. This implies that the load resistance should match the internal resistance for the best results.

We then proceeded with these constraints as input data for the computer program in order to get the resulting output power and efficiency.

5. Results

We consider the parametric properties of materials in our optimization analysis. The effects of material on elec-

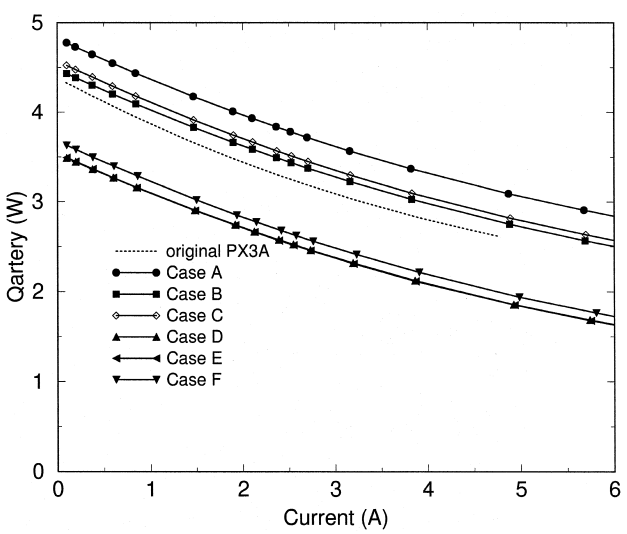

Fig. 6. Conducted heat to condenser through artery.

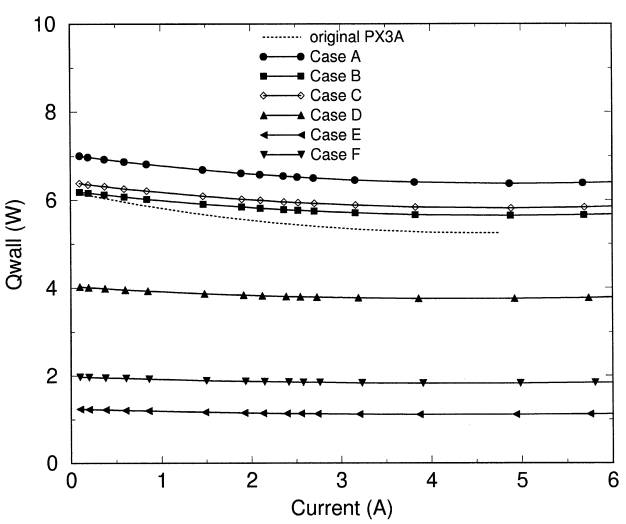

Fig. 7. Conducted heat to condenser through cell wall.

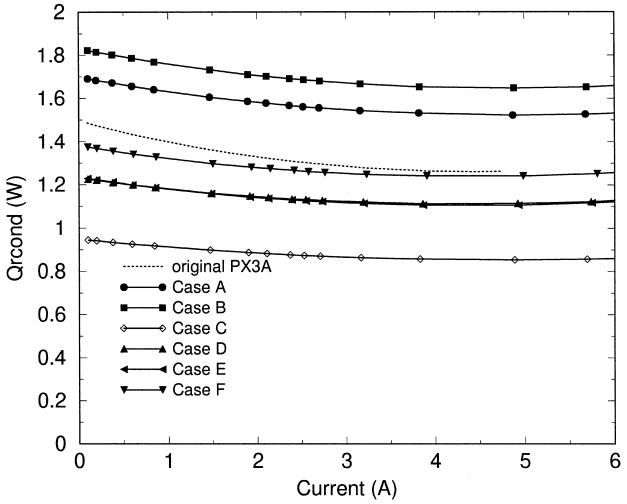

Fig. 8. Radiation heat losses from condenser.

trical power generated by the PX-3A cell, the amount of the heat supplied to the cell, the efficiency of the cell, and the losses from the cell are given in Figs. 2–9. The temperature maintained at the hot plate is 1173 K, and at the condenser side is 623 K for all these cases. In these figures, the dotted line shows the values for the original PX-3A cell.

The maximum power generated by the cell is given in Table 2. Some other relevant parameters for the maximum power are given in the same table. Also, heat losses are given as the percentage of the Q_{input}. The following material changes are made for the cell to compare the results:

Case A: material for hot plate, stud and evaporator is changed from SS to Ni.

Case B: in addition to case A, the material for condenser, artery, shield and cell wall is changed from SS to Inconel.

Case C: in addition to case B, the emissivity of sodium film is changed from 0.05 to 0.025; because the emissivity of liquid sodium is given as 0.02 in Ref. [51].

Case D: in addition to case C, cell wall and artery coated with Rh ($\varepsilon = 0.06$).

Case E: in addition to case D, material for cell wall above the BASE tube is changed from SS to ceramic, ZrO_2.

Case F: in addition to case E, perfect insulator is assumed as an insulation material instead of Molded Mink-K.

In Fig. 2, it can be seen that the electrical power generated by the cell increases appreciably for case A. In this case, the maximum power reaches from 4.49 W to 5.97 W. For cases B, C, D, E and F, the electrical power increases slowly. The maximum power in case F is obtained as 6.26 W. Heat input to the cell vs. current is given in Fig. 3. The maximum heat goes into the cell in case A because Ni has a higher thermal conductivity than SS. For case B, the amount of heat supplied to the cell, Q_{input}, decreases because of the Inconel's lower thermal conductivity which impedes the loss of heat through walls and condenser. Depending on heat losses, Q_{input} goes down for cases C, D, E and F; and it takes the minimum values in case F.

The cell conversion efficiency vs. current is given in Fig. 4. The maximum efficiency is 12.98% for the original cell, the maximum efficiencies for cases A through F are substantially increased around the current 2–2.5 A. They are given in Table 3. Heat losses through cell wall and insulation, Q_{insul}, through artery, Q_{artery}, and through cell wall, Q_{wall}, are given in Figs. 5–7. They show higher values from the original cell in cases A, B and C, but smaller values in cases D, E and F. Heat loss in case F is minimum for Q_{insul}, but in the case of Q_{artery} and Q_{wall}, the minimum is for case E. In case F, the perfect insulator is assumed for insulation material. It means that there is no heat losses through the cell wall and insulation. That time

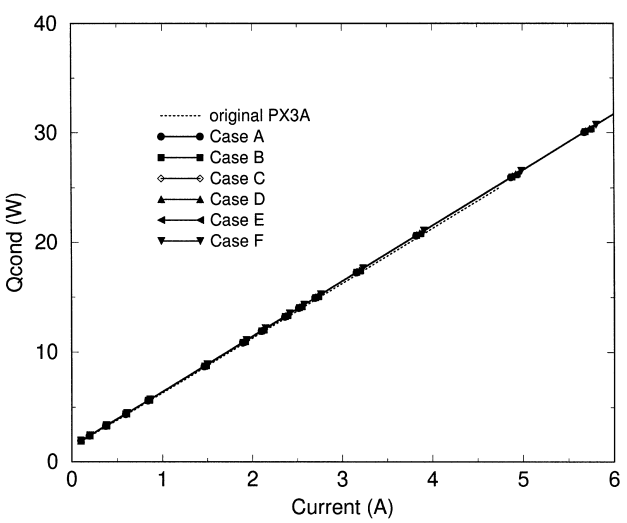

Fig. 9. Latent heat of condensation of sodium.

Table 2
Comparison of heat losses at the maximum power generated by the AMTEC cell

	Original	Case A	Case B	Case C	Case D	Case E	Case F
$P_{out,max}$ (W)	4.490	5.971	5.995	6.012	6.109	6.135	6.253
I (A)	2.447	3.155	3.161	3.166	3.191	3.198	3.228
η (%)	12.642	13.917	14.278	14.484	15.866	17.067	20.789
Q_{input} (W)	35.514	42.901	41.987	41.511	38.507	35.944	30.078
Q_{insull} (W)	7.079	7.492	7.487	7.518	7.099	7.118	0.0
Q_{artery} (W)	3.257	3.550	3.207	3.281	2.299	2.291	2.395
Q_{wall} (W)	5.415	6.423	5.674	5.848	3.746	1.115	1.833
Q_{rcond} (W)	1.300	1.536	1.659	0.860	1.117	1.110	1.246
Q_{cond} (W)	13.495	17.238	17.273	17.298	17.438	14.474	17.643
Q_{insul} (%)	19.932	17.465	17.831	18.112	18.436	19.804	0.0
Q_{artery} (%)	9.170	8.275	7.639	7.904	5.970	6.374	7.962
Q_{wall} (%)	15.247	14.973	13.951	14.088	9.729	3.103	6.095
Q_{rcon} (%)	3.662	3.581	3.951	2.072	2.900	3.088	4.143
Q_{cond} (%)	38.000	40.180	41.139	41.671	45.286	48.615	58.656

Table 3
Comparison of maximum conversion efficiency of the AMTEC cell

	Original	Case A	Case B	Case C	Case D	Case E	Case F
I (A)	1.98	2.52	2.52	2.44	2.39	2.32	1.93
η_{max} (%)	12.98	14.38	14.79	15.02	16.64	18.09	22.99
Improvement in efficiency (%)	–	10.79	13.94	15.72	28.20	39.37	77.12
Minimum BASE temperature (K)	1062	1088	1091	1093	1108	1110	1126
Maximum BASE temperature (K)	1141	1153	1153	1154	1156	1157	1161
Minimum shield temperature (K)	898	928	945	954	1010	1012	1062
Maximum shield temperature (K)	1003	1045	1050	1054	1076	1050	1103
Wall temperature at certain point (K)	1049	1106	1110	1111	1122	1138	1153

temperatures of the cell elements (wall, evaporator, BASE tube, artery, . . .) become higher (Table 3). Therefore, Q_{artery} and Q_{wall} will increase when Q_{insul} become zero. As the conducted heat losses through the artery for cases D and E are almost the same, the conducted heat losses through the cell wall for cases D and E show a big difference. Because the ceramic material ZrO_2 is considered only for cell wall not for artery in case E. The ZrO_2 has lower thermal conductivity than SS has (for ZrO_2 2.5 W/mK and for SS 25 W/mK at 1000 K). The net heat radiation to condenser increases for cases A and B, but it decreases for other cases compared to the original cell. Depending on the low sodium film emissivity ($\varepsilon = 0.025$), it takes the smallest values in case C. Although the sodium film emissivity is the same for cases D, E and F, Q_{rcond} increases because of higher temperatures of the cell elements (Fig. 8). The condensation heat losses, Q_{cond}, have almost the same values in all cases as should be expected (see Fig. 9).

6. Conclusion

We have been able to reduce the losses almost on all counts thereby increasing the output power and thus the efficiency of AMTEC. The efficiency has improved considerably when we incorporate the variation in the material used in the cell. Moreover, we make the following recommendations:

- The interior cell wall could be coated with some appropriate material with high reflective coefficient and low emissivity.
- The cell wall could be made of double layers with air in between.
- The artery's outer surface should be coated with the same material used for the cell wall coating.
- Condenser may be coated with sodium also.
- The power output maximizes at a certain value of the current in the circuit, and when the load resistance matches the internal resistance of the cell. For best results, the cell must be operated under those conditions.
- For conductive losses through the wall, artery and insulation, low thermal conductive materials must be used, but for hot plate high thermal conductivity material is recommended.

7. List of symbols

A_{artery}	cross-section area of artery (m^2)
A_{wall}	cross-section area of wall (m^2)
F	Faraday's constant (96,485 C/mole)
F_{ij}	view factor between surfaces i and j
h_{fg}	latent heat of condensation of sodium per unit mass (J/kg)
I	cell current (A)
J	current density (A/m^2)
k	thermal conductivity (W/mK)
K	coefficient includes conduction and radiation effects (W/m^2K)
$\dot{m}$	sodium flow rate (kg/s)
P	perimeter of cell wall (m)
P_a	pressure at anode side (Pa)
P_c	pressure at cathode side (Pa)
P_{out}	electrical energy generated by the cell (W)
Q_{air}	heat passes the air as cooling fluid (W)
Q_{artery}	conducted heat to condenser through artery (W)
Q_{cold}	heat loss at the edge of cold plate (W)
Q_{cond}	latent heat of condensation of sodium (W)
Q_{insul}	heat losses to ambient through cell wall and insulation (W)
Q_{loss}	total heat losses (W)
Q_{rcond}	net radiated energy to condenser (W)
Q_{wall}	conducted heat to condenser through cell wall (W)
R	perfect gas constant (8.314 J/mol K)
R_{bus}	electrical resistance of bus wire (Ωm^2)
R_B	ionic electrical resistance (Ωm^2)
$R_{collector}$	electrical resistance of current collector (Ωm^2)
$R_{contact}$	contact resistance of the electrodes (Ωm^2)

R_{int}	total internal resistance (Ωm^2)
R_{op}	charge exchange polarization loss (Ωm^2)
R_{sheet}	sheet resistance in the plane of electrode (Ωm^2)
t_B	thickness of BASE tube (m)
T	temperature (K)
V	cell voltage (V)
V_{oc}	cell voltage in open-circuit
V_{op}	electrode polarization over potential (V)
x	distance from condenser (m)
Greek	
ε	emissivity
η	cell conversion efficiency
ρ_B	electrical resistivity (Ωm)
ζ^a	electrode polarization over potential at anode (V)
ζ^c	electrode polarization over potential at cathode (V)

Acknowledgements

We are indebted to Clay Mayberry and John Meril for Providing the AMTEC data before publication and Dr. Jean-Michel Tournier for many useful discussions. This work is based in part on work supported by the Center for Energy Research, Texas Tech University, Texas Advanced Technology Program under Grant No. 003644-091, and AFOSR Sub-contract 99-0832 CFDA #12.800.

References

[1] J.T. Kummer, N. Weber, U.S. Patent 3,458,356, assigned to Ford Motor, 1968.
[2] N. Weber, Energy Convers. 14 (1974) 1.
[3] T.K. Hunt, N. Weber, T. Cole, in: Proceeding of the 13th Intersociety Energy Conversion Engineering Conference, SAE, Warrandale, PA, 1978, p. 2001.
[4] T.K. Hunt, N. Weber, T. Cole, in: J.B. Bates, G.C. Ferrington (Eds.), Solid State Ionics, North-Holland, Amsterdam, 1981, p. 263.
[5] T. Cole, Science 221 (1983) 915.
[6] R. Ewell, J. Mondt, in: M.S. El-Genk, M.D. Hoover (Eds.), Space Nuclear Power Systems 1984, Orbit Book, Malabar, FL, 1985, p. 385.
[7] C.P. Bankston, T. Cole, S.K. Khanna, A.P. Thakoor, in: M.S. El-Genk, M.D. Hoover (Eds.), Space Nuclear Power Systems, Orbit Book, Malabar, FL, 1985, p. 393.
[8] R.C. Dahlberg et al., in: M.S. El-Genk (Ed.), Review of Therrnionic Technology 1983 to 1992, A Critical Rev of Space Nuclear Power and Propulsion 1984–1992, AIP Press, New York, 1994, pp. 121–161.
[9] A. Shock, in: Proc. 15th Intersociety Energy Conversion Engineering Conference, Vol. 2, AIAA, New York, 1980, p. 1032.
[10] D. Birden, F.A. Angelo, in: Proc. 18th Intersociety Energy Conversion Engineering Conference, AIChE, New York, 1983, p. 61.
[11] E.J. Brat, G.O. Fitzpatrick, Direct Conversion Nuclear Reactor Space Power Sy., Report No. AFWALTR-82-2073, Vol. 1.
[12] R.M. Williams, B. Jeffries-Nakamura, M. Underwood, B. Wheeler, M. Loveland, S. Kikkert, J. Lamb, T. Cole, J. Kummer, C.P. Bankston, J. Electrochem. Soc. 136 (1989) 893.
[13] R.M. Williams, M.E. Loveland, B. Jeffries-Nakamura, M.L. Underwood, C.P. Bankton, H. Leduc, J.T. Kummer, J. Electrochem. Soc. 137 (1990) 1709.
[14] R.M. Williams, B. Jeffries-Nakamura, M.L. Underwood, C.P. Bankton, J.T. Kummer, J. Electrochem. Soc. 137 (1990) 1716.
[15] M.A. Ryan, B. Jeffries-Nakamura, R.M. Williams, M.L. Underwood, D. O'Connor, S. Kikkert, Proceedings of the 26th Intersociety Energy Conversion Engineering Conference, Am. Nucl. Soc. 5 (1991) 463.
[16] M.A. Ryan, R.M. Williams, B. Jeffries-Nakamura, M. L. Underwood, D. O'Connor, JPL New Technology Report, 18620-8166, 1991.
[17] M.A. Ryan, B. Jeffries-Nakamura, D. O'Connor, M.L. Underwood, R.M. Williams, in: D.D. Macdonald, A.C. Khanker (Eds.), Proc. Symposium on High Temperature Electrode Materials and Characterization, Electrochem. Soc., 91 (1991) 115.
[18] C.B. Vinning, R.M. Williams, M.L. Underwood, M.A. Ryan, J.W. Suiter, Proceedings of the 27th Intersociety Energy Conversion Engineering Conference, SAE 3 (1992) 123.
[19] M.L. Underwood, R.M. Williams, M.A. Ryan, B. Jeffries-Nakamura, D. O'Connor, in: M.S. El-Ghenk, M.D. Hoover (Eds.), Proc. 9th Symp. On Space Nuclear Power Systems, Am. Inst. Phys., 3 (1992) 1331.
[20] M.L. Underwood, D. O'Connor, R.M. Williams, B. Jeffries-Nakamura, M.A. Ryan, in: Proc. 27th IECEC, 3 (1992) 197.
[21] M.L. Underwood, B. Jeffries-Nakamura, D. O'Connor, M.A. Ryan, J.W. Suitar, R.M. Williams, in: Proc. 28th IECEC, 1 (1993) 855.
[22] M.A. Ryan, R.M. Williams, B. Jeffries-Nakamura, M.L. Underwood, D. O'Connor, NASA Tech. Briefs, 1993, p. 80.
[23] M.A. Ryan, R.M. Williams, C. Spaipetch, A. Kisor, D. O'Connor, M.L. Underwood, B. Jeffries-Nakamura, CONF940101, AIP Press, New York, 1994, p. 1495.
[24] M.A. Ryan, A. Kisor, R.M. Williams, B. Jeffries-Nakamura, D. O'Connor, in: Proc. 29th IECEC, 2 (1994) 877.
[25] M.A. Ryan, R.M. Williams, M.L. Phillips, L. Lora, J. Miller, in: M.S. El-Ghenk (Ed.), Proc. Space Technology and Applications International Forum — 1998, AIP Press, New York, 1998, p. 1607.
[26] R.K. Sievers, T.K. Hunt, J.F. Ivanenok, J. Pantolin, D.A. Butkiewicz, in: M.S. El-Genk, M.D. Hoover (Eds.), Proc. 10th Space Nuclear Power and Propulsion, CONF-930103, AIP Press, New York, 1993, p. 319.
[27] R.K. Sievers, J.R. Rasmussen, C.A. Barkowski, T.J. Hendricks, J.E. Pantolin, in: Proc. STAIF-98, CONF-980103, AIP Press, New York, 1998, p. 1479.
[28] M.J. Schuller, P. Haugen, E. Reiners, J. Merrill, R.K. Sievers, R. Svedberg, J.F. Ivanenok III, C.J. Crowley, M.G. Izenson, in: Proc. 31st IECEC, IEEE, paper no. 96184, Vol. 2, 1996, p. 877.
[29] J. Merrill, M.J. Schuller, R.K. Sievers, C.A. Borkowski, L. Huang, M.S. El-Genk, in: Proc. 32nd IECEC, IEEE, paper no. 97379, Vol. 2, 1997, p. 1184.
[30] J.M. Merrill, M. Schuller, L. Huang, in: M.S. El-Genk (Ed.), Proc. STAIF, CONF-980103, AIP Press, New York, 1998, p. 1613.
[31] A. Schock, in: Proc. 15th Intersoc. Energy Conversion Engineering Conf., 1980, p. 1032.
[32] A. Schock, H. Norivan, C. Or, V. Kumar, in: Proc. 48th Intl. Astronomical Congress, 1997, p. 1.
[33] A. Schock, H. Norivan, C. Or, V. Kumar, Preprint for presentation in 33rd Intesoc. Energy Conversion Engineering Conf., 1998.
[34] J.M. Tournier, M.S. El-Ghenk, in: Proc. 15th STAIF, AIP Press, New York, 1998, p. 1576.
[35] A. Kato, Nakata, K. Tsuchida, in: Proc. 27th IECEC, Am. Chem. Soc., paper No. 929006, 1992, p. 1.
[36] A. Kato, Nakata, K. Tsuchida, in: Proc. 28th IECEC, Am. Chem. Soc., paper no. 93027, 1993, p. 809.
[37] C.J. Crowley, M.G. Izenson, in: M.S. El-Genk (Ed.), Proc. 10th Symp. On Space Nuclear Power and Propulsion, CONF-930103, AIP Press, New York, 1993, p. 897.

[38] M.G. Izenson, C.J. Crowley, Proceedings of the 28th Intersociety Energy Conversion Engineering Conference, Am. Chem. Soc. 1 (1993) 829, Paper no. 93221.
[39] M.G. Izenson, C.J. Crowley, Proceedings of the 31st Intersociety Energy Conversion Engineering Conference, IEEE 4 (1996) 2226, Paper no. 96262.
[40] M. Sayer, M.F. Bell, B.A. Judd, J. Appl. Phys. 67 (1990) 832.
[41] M.L. Underwood, D. O'Connor, R.M. Williams, M.A. Ryan, C.P. Bankston, J. Propul. Power 8 (1993) 878.
[42] M.L. Underwood, R.M. Williams, M.A. Ryan, B. Jeffries-Nakamura, in: M.S. El-Genk, M.D. Hoover (Eds.), Proc. Space Nuclear Power and Propulsion, CONF-930103, AIP Press, New York, 1993, p. 885.
[43] A. Schock, H. Noravian, V. Kumar, C. Or, in: Proc. 32nd Interdisciplinary Energy Conversion Conf., #97529, Vol. 2, 1997, p. 1136.
[44] M.A.K. Lodhi, M. Schuller, P. Housgen, in: M.S. El-Genk (Ed.), Proc. Space Technology and Applications International Forum, AIP Press, New York, 1996, p. 1285.
[45] M.S. El-Ghenk, J-M. Tournier, in: Proc. 5th ESPC-98, 416 (1998) 257.
[46] H. Noravian, in: Proc. 26th International Conference on Environmental Systems, No. 961376, 1996.
[47] J. Gaski, SINDA (System Improved Numerical Differencing Analyzer), vers. 1.315 from Network Analysis Associate, Fountain Valley, CA, 1987.
[48] A.M. Straus, S.W. Peterson, in: Proc. STAIF, 1998, p. 1571.
[49] M. Steinbruck, V. Heinzel, F. Huber, W. Pepler, in: Proc. 28th IECEC I.1, 799, 1993.
[50] C.J. Crowly, M.G. Izenson, P.N. Wallis, R.K. Sievers, J.F. Ivanenok III, in: Proc. 29th IECEC, Vol. 1, AIAA, 1994, p. 882.
[51] J.M. Tournier, M.S. El-Ghenk, M. Schuller, P. Hausgen, in: Proc. 14th STAIF-97, 397, 1997.